

Rotational state modification and fast ortho-para conversion of H₂ trapped within the highly anisotropic potential of Pd(210)

S. Ohno,¹ D. Ivanov,¹ S. Ogura,¹ M. Wilde,¹ E. F. Arguelles,² W. A. Diño,^{2,3} H. Kasai,⁴ and K. Fukutani^{1,*}

¹*Institute of Industrial Science, The University of Tokyo, Komaba, Meguro-ku, Tokyo, 153-8505, Japan*

²*Department of Applied Physics, Osaka University, Suita, Osaka 565-0871, Japan*

³*Center for Atomic and Molecular Technologies, Osaka University, Suita, Osaka 565-0871, Japan*

⁴*National Institute of Technology, Akashi, Nishioka, Uozumi-cho, Akashi, Hyogo 674-8501, Japan*

 (Received 18 October 2017; revised manuscript received 27 December 2017; published 26 February 2018)

The rotational state and ortho-para conversion of H₂ on a Pd(210) surface is investigated with rotational-state-selective temperature-programmed desorption (RS-TPD) and theoretical calculations. The isotope dependence of TPD shows a higher desorption energy for D₂ than that for H₂, which is ascribed to the rotational and zero-point vibrational energies. The RS-TPD data show that the desorption energy of H₂($J = 1$) (J : rotational quantum number) is higher than that of H₂($J = 0$). This is due to the orientationally anisotropic potential confining the adsorbed H₂, which is in agreement with theoretical calculations. Furthermore, the H₂ desorption intensity ratio in $J = 1$ and $J = 0$ indicates fast ortho-para conversion in the adsorption state, which we estimate to be of the order of 1 s.

DOI: [10.1103/PhysRevB.97.085436](https://doi.org/10.1103/PhysRevB.97.085436)

I. INTRODUCTION

Molecular hydrogen, the most common molecule in the universe, exhibits unique characters and features. Of particular interest and importance are H₂ quantum rotation and nuclear-spin modifications. H₂ occurs in two nuclear-spin isomeric forms of ortho-H₂ and para-H₂ with antiparallel ($I = 0$) and parallel ($I = 1$) proton spins, respectively, with I the quantum number of the total nuclear spin. Due to symmetry restrictions, we can only find ortho-H₂ in odd J states and para-H₂ in even J states [1,2]. In the gas phase, interconversion between these two isomeric species occurs with negligible probability [3]. This allows us to treat them as if they were different molecules.

When H₂ physisorbs weakly on a surface via van der Waals interaction, it retains its nearly free-rotational motion as confirmed by electron energy loss spectroscopy (EELS) [4–7] and inelastic electron tunneling spectroscopy [8–12]. On the other hand, H₂ may be molecularly chemisorbed (MC) on particular surfaces [13–16]. A previous TPD study on Pd(210) shows H₂ desorption temperature is as high as 80 K, and a significant chemical interaction between H₂ and Pd is recognized by density functional theory (DFT) calculations [16,17]. As a consequence, H₂-surface interactions may manifest as a strongly anisotropic potential confining H₂ inducing rotational modifications and ortho-H₂ to para-H₂ (o-p) conversion [1,2,18].

Previous EELS studies suggest that H₂ adsorbed at the step site of Cu(510) rotates two dimensionally and undergoes fast o-p conversion [14,15,19]. However, the potential could be highly anharmonic, and the modification of the rotational-energy level potentially affects the o-p conversion time, because the o-p conversion is accompanied by rotational-energy

dissipation. In these regards, the rotational motion and o-p conversion mechanism in the MC state are yet to be elucidated. The ubiquitous stepped surfaces especially in nanostructures and confined spaces provide us with a good playground to further study the rotational state of adsorbed H₂ and the accompanying o-p conversion [8,9,11,12,20,21].

Here we report the results of RS-TPD on H₂/Pd(210). In RS-TPD, the thermal desorption intensity is recorded for specific J states, and it has been shown that RS-TPD is a powerful method to investigate the rotational state and o-p conversion [22–24]. Our results show a blueshift in the corresponding RS-TPD data for $J = 1$ as compared to $J = 0$. This indicates a more stable $J = 1$ adsorption as compared to $J = 0$. The intensity ratio of the two RS-TPD data plotted as a function of temperature exhibits an Arrhenius relation below 75 K reflecting thermal equilibrium between the ortho and para states. On the other hand, the ratio shows a substantial deviation from the relation expected from the thermal equilibrium above 75 K. We estimate the o-p conversion time to be of the order of 1 s.

II. EXPERIMENTAL AND THEORETICAL METHODS

The experiments were performed under ultrahigh vacuum conditions. The Pd(210) surface was cleaned by repeated cycles of Ar ion sputtering, annealing at 1000 K, annealing at 750 K under an O₂ pressure of 5×10^{-5} Pa followed by cooling in H₂ of 5×10^{-5} Pa, and final flashing at 600 K until a clear low-energy electron diffraction pattern was observed [25]. After exposing the clean Pd(210) surface to H₂(D₂) at 50 K, TPD data were taken with a ramp rate of 2.8 K s⁻¹. While a shielded quadrupole mass spectrometer (QMS) was used for conventional TPD, RS-TPD was carried out using the (2+1) resonance-enhanced multiphoton ionization via the $E, F^1\Sigma_g^+$ states, which allows for the J -state selective detection of H₂

*fukutani@iis.u-tokyo.ac.jp

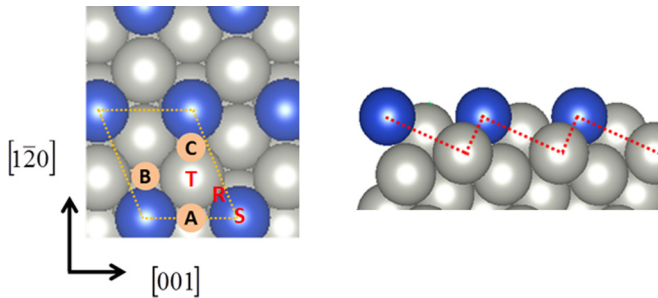


FIG. 1. Top (left) and side (right) views of the Pd(210) surface. The unit cell is shown by the dashed lines (left). The surface consists of steps and terraces, where the step atom is indicated by blue color. A–C and R–S denote possible adsorption sites of hydrogen.

[2,26]. The RS-TPD data were taken for several times for each J , and the peak temperature was confirmed to be reproduced within 0.3 K. Para-rich H_2 was produced by a homemade o-p conversion cell using an iron oxide catalyst [27]. Unless otherwise stated, H_2 (D_2) dosage refers to normal H_2 (D_2) dosage with an ortho-para ratio of 3 (2).

Figure 1 shows the structure of the Pd(210) surface with possible adsorption sites denoted as A–C and R–T. According to DFT calculations [16,17,27], H_2 is dissociatively adsorbed at the A site at a low coverage, and then H_2 is molecularly chemisorbed at the S site of the H-precovered surface. The eigenstate energies in the MC state were obtained by numerically solving the Schrödinger equation for the rotational and Z motion of H_2 (Z: the center-of-mass position of H_2 from the surface) under the potential obtained by DFT calculations with the H–H bond length fixed [27]. Although the potential obtained by DFT calculations contain an uncertainty of about 10 meV, the relative energy between H_2 and D_2 and between the rotational states may be compared within approximately 1 meV. The energy values are therefore described to the first decimal place below.

III. RESULTS AND DISCUSSION

As described above, hydrogen is initially adsorbed in a dissociative way followed by molecular chemisorption. The QMS-TPD data show distinct features at 200–350 K for small H_2 dosage (cf. Fig. S1 [27]), which correspond to H atoms dissociatively adsorbed on the surface [16]. After saturation of these features, an additional low-temperature peak starts to develop at approximately 80 K with increasing dosage. Figure 2 shows the QMS-TPD data in the low-temperature region taken after H_2 (D_2) dosages of 0.36–0.57 (0.45–0.78) Langmuir (1 Langmuir = 1.33×10^{-4} Pa s). For H_2 , a desorption peak is observed at approximately 80 K that shifts to lower temperature with increasing dosage. For D_2 , on the other hand, a slightly blueshifted desorption peak is seen as compared to the results for H_2 . A TPD measurement after coadsorption of H_2 and D_2 showed no HD signal in the low-temperature region confirming the molecularly adsorbed nature of this species in agreement with a previous study [16]. Furthermore, any indication of hydrogen exchange between the dissociatively adsorbed H(D) and $H_2(D_2)$ in the MC state was not observed within the experimental time scale. The shift of the TPD peak to the

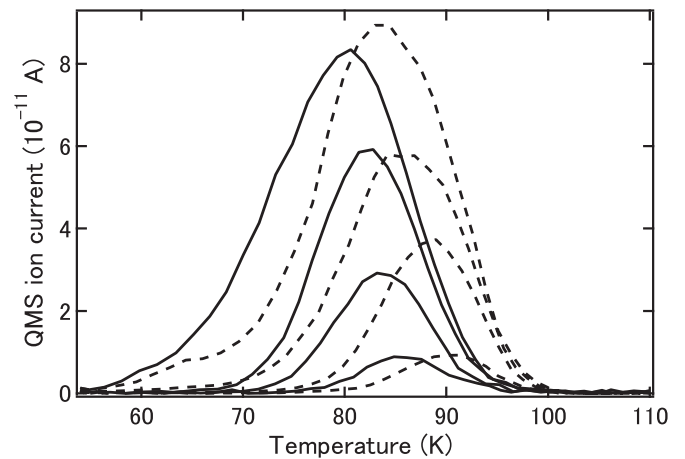


FIG. 2. QMS-TPD in the low surface temperature region after 0.36, 0.39, 0.47, and 0.57 Langmuir H_2 exposures (solid curves, from bottom to top) and after 0.45, 0.56, 0.65, and 0.78 Langmuir D_2 exposures (dashed curves, from bottom to top).

lower-temperature region with increasing coverage suggests repulsive interaction between adsorbed $H_2(D_2)$. Evaluation of the desorption energy from the TPD peak temperature on the basis of the Redhead formula needs the frequency factor [36]. The difference of the desorption energy between H_2 and D_2 , however, does not depend on the choice of the frequency factor, and can be estimated to be 7 ± 1 meV at saturation coverage [27].

Figure 3 shows the RS-TPD data for the $J = 0$ and $J = 1$ states recorded 120 s after saturation of the H_2 MC state at 50 K. While the $J = 1$ desorption curve reveals a peak at 78 K, the data of $J = 0$ shows a peak at 74 K, which is clearly lower than that of $J = 1$. Note that no signal for $J \geq 2$ was observed. This is because a $J = 0 \rightarrow 2$ ($J = 1 \rightarrow 3$) rotational excitation in the gas phase requires an energy of 45(75) meV, which leads to negligible thermal populations in $J \geq 2$ at the desorption temperature of ~ 80 K. These results suggest that ortho- H_2 and para- H_2 are in their lowest adsorption states. It is also

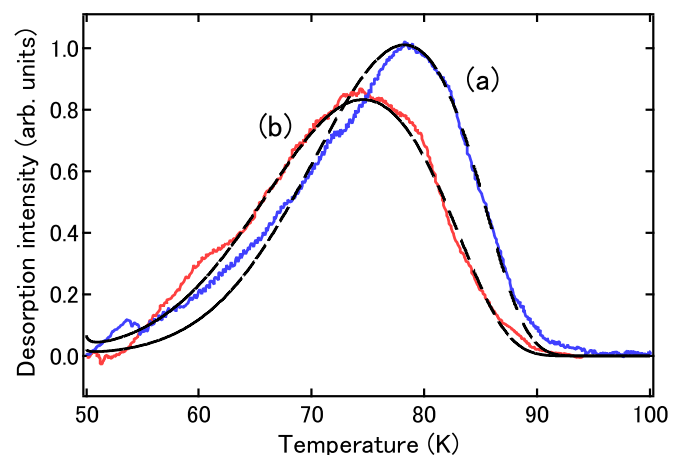


FIG. 3. H_2 RS-TPD of (a) $J = 1$ (blue) and (b) $J = 0$ (red) in the low-temperature region after a 0.57 Langmuir dosage. Dashed curves show numerically simulated TPD.

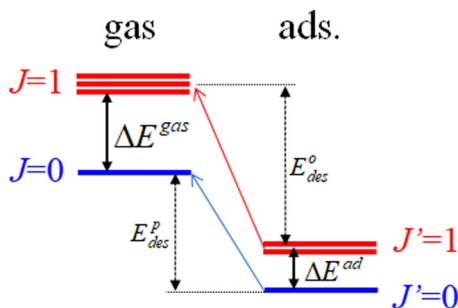


FIG. 4. Energy diagram in the gas phase and adsorption state of H₂ in the respective $J(J')$ states. The energy difference between the $J(J') = 1$ and $J(J') = 0$ states is denoted by ΔE^{gas} (ΔE^{ad}), and the desorption energy for the $J = 1(0)$ state is indicated by $E_{\text{des}}^{\text{o(p)}}$.

noted that the average desorption temperature of the two data in Fig. 3 is slightly lower than that of Fig. 2 probably because of the slightly different setup for QMS-TPD and RS-TPD.

As discussed in the literature [24,37], the blueshift of the $J = 1$ TPD data compared to that of $J = 0$ can be attributed to the lifting of the rotational-state degeneracy due to the anisotropic adsorption potential. Under the anisotropic potential, because of rotational symmetry breaking, the gas phase rotational states no longer describe the eigenstates of the adsorption state. This leads to modifications in the corresponding rotational energies and wave functions. When the anisotropic potential is sufficiently small compared to the rotational energy (14.7 meV for $J = 1$), the deviation of the rotational energy may be treated within the perturbation theory. While the energy of the $J = 0$ state remains unchanged, the degeneracy of the triply degenerate $J = 1$ states is lifted [24,37].

The adsorption potential of H₂ in the MC state on Pd(210) at a coverage of one monolayer ($5.91 \times 10^{14} \text{ cm}^{-2}$) was obtained by DFT-based total energy calculations. As shown in Fig. S3, the potential energy is displayed as a function of Z with the molecular axis fixed at certain directions [27]. The energy profile shows strong polar (θ) anisotropy (~ 200 meV) and negligible azimuthal (ϕ) anisotropy (< 1 meV) for the H₂ molecular-axis orientation. Furthermore, the potential reveals an anharmonic dependence on Z . These results imply that rotational-state analyses based on perturbation theory do not hold [37,38]. The eigenstate in the MC state was therefore obtained by solving the Schrödinger equation for the molecular motion of H₂ under the potential obtained by DFT calculations. The obtained eigenenergy $E_{J'}^{\text{ad}}$ is $E_{J'=0(1)}^{\text{ad}} = -202.3(-197.6)$ meV for adsorbed H₂ in the $J' = 0(1)$ rotational state. Here the eigenstate in the adsorption is described by J' to distinguish from the gas-phase rotational state J , because the angular momentum of H₂ is not a good quantum number due to the strong θ anisotropy and Z anharmonicity. The energy diagram for the gas phase and adsorption state is shown in Fig. 4. While the $J = 1$ state is triply degenerate, the $J' = 1$ state is doubly degenerate. The corresponding wave function for $J' = 0(1)$ shows even (odd) character with respect to space inversion allowing us to assign $J' = 0(1)$ to para-(ortho-) species. Correspondingly, for adsorbed D₂, we obtain $E_{J'=0(1)}^{\text{ad}} = -214.5(-210.7)$ meV.

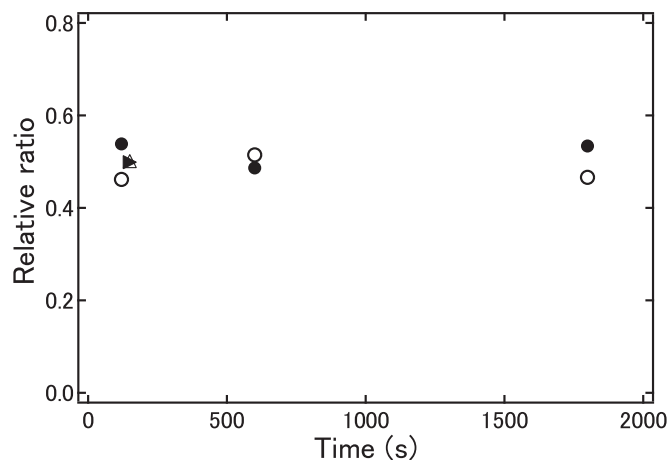


FIG. 5. Relative intensity of the integrated RS-TPD for $J = 1$ (filled circles) and $J = 0$ (open circles) after normal-H₂ dosage measured at various residence times. Experimental data after dosage of para-rich H₂ are also shown by filled ($J = 1$) and open ($J = 0$) triangles.

To determine the desorption energy, we need to take into account zero-point vibrations (ZPV) in the surface parallel direction and the internal stretch mode. From the harmonic approximation, the ZPV of H₂ in the former and latter is calculated to be 27.3 and 202 meV, respectively, whereas the ZPV of the internal stretch in the gas phase is obtained to be 259.5 meV. Note that the bond length of H₂ is slightly elongated due to the chemical interaction, which modifies the rotational constant. However, its effect on the rotational energy is smaller than the potential effect [21]. Assuming the ZPV of D₂ to be smaller than that of H₂ by a factor of $\frac{1}{\sqrt{2}}$, desorbing H₂(D₂) from the adsorbed $J' = 0$ to the gas phase $J = 0$ state requires an energy of 232.6(235.9) meV. Desorbing H₂ from the $J' = 1$ to $J = 1$, on the other hand, requires 242.6 meV. The energy differences of 3.3 meV between H₂ and D₂ and 10.0 meV between $J = 1$ and $J = 0$ are roughly consistent with the experimental results of Figs. 2 and 3.

The RS-TPD data of $J = 0$ and $J = 1$ in Fig. 3 have similar integrated intensities. For comparison, note that normal-H₂ has an o-p ratio of 3. Figure 5 shows the evolution of the desorption intensities in $J = 0$ and 1 measured by RS-TPD as a function of the residence time of H₂ on the surface. This shows that the intensity ratio of $J = 1/J = 0$ does not change within 2000 s. Previous studies on Ag and ice surfaces showed a substantial decrease in the $J = 1/J = 0$ ratio, which was attributed to o-p conversion taking place in the adsorption state [23,26,39]. To determine whether or not o-p conversion occurs, RS-TPD experiments were carried out using 95% para-H₂ (5% ortho-H₂). After a dosage of 0.7 Langmuir para-rich H₂, the subsequent RS-TPD recorded after a surface residence time of 150 s shows similar intensities for $J = 1$ and $J = 0$, which are also plotted in Fig. 5. This strongly suggests that the o-p conversion time is much shorter than 150 s, and that the populations of the $J' = 0$ and $J' = 1$ states shown in Fig. 4 are in thermal equilibrium. It should be noted that the RS-TPD data

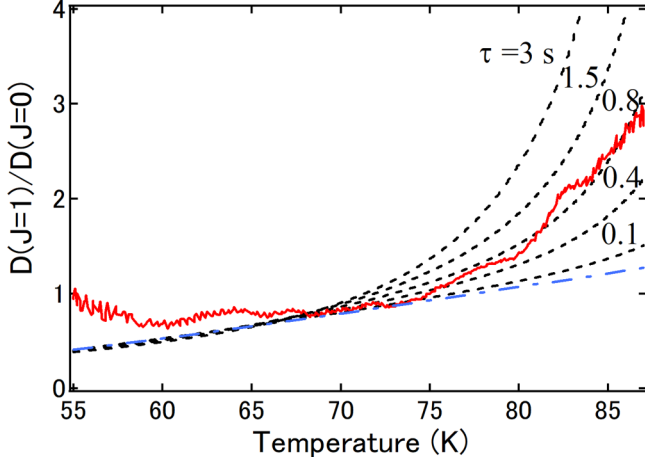


FIG. 6. Desorption intensity ratio of $J = 1$ to $J = 0$ as a function of surface temperature (red solid curve). Relation expected assuming thermal equilibrium between the $J = 1$ and $J = 0$ states in the adsorption (blue dot-dashed curve) and numerically simulated relations for various o-p conversion time τ (black dashed curves).

did not change when the adsorption temperature was changed between 36 and 54 K.

In Fig. 6 we show how the ratio of the desorption intensity $D(J)$ in $J = 1$ and $J = 0$, which is obtained from the data shown in Fig. 3, changes with the surface temperature. This shows a gradual increase up to 75 K followed by a steep increase above 75 K. To understand this behavior, we suppose that the o-p conversion is so fast that the populations $P(J')$ in the $J' = 1$ and $J' = 0$ states shown in Fig. 4 are in thermal equilibrium in the adsorption state. Then

$$\frac{P(J' = 1)}{P(J' = 0)} = \frac{g_{l=1} g_{J'=1}^{\text{ad}}}{g_{l=0} g_{J'=0}^{\text{ad}}} \exp\left(-\frac{\Delta E^{\text{ad}}}{k_B T_S}\right) \quad (1)$$

gives an expression for the population ratio of $J' = 1$ and $J' = 0$ in terms of the nuclear spin degeneracy g_l and rotational state degeneracy $g_{J'}^{\text{ad}}$ in the adsorption state with the Boltzmann constant k_B and the surface temperature T_S [27]. $\Delta E^{\text{ad}} = E_{J'=1}^{\text{ad}} - E_{J'=0}^{\text{ad}}$ is the energy difference between the $J' = 1$ and $J' = 0$ states. According to the present theoretical calculations, $\Delta E^{\text{ad}} = 4.7$ meV.

Similarly,

$$\begin{aligned} \frac{D(J = 1)}{D(J = 0)} &= \frac{P(J' = 1)}{P(J' = 0)} \frac{(g_{J=1}^{\text{gas}}/g_{J=1}^{\text{ad}})}{(g_{J=0}^{\text{gas}}/g_{J=0}^{\text{ad}})} \exp\left(-\frac{\Delta E^{\text{gas}} - \Delta E^{\text{ad}}}{k_B T_S}\right) \\ &= \frac{g_{l=1} g_{J=1}^{\text{gas}}}{g_{l=0} g_{J=0}^{\text{gas}}} \exp\left(-\frac{\Delta E^{\text{gas}}}{k_B T_S}\right) \end{aligned} \quad (2)$$

gives an expression for the ratio of the desorption intensity [27]. Here g_J^{gas} is the degeneracy of the rotational state in the gas phase, and $g_{J=1}^{\text{gas}}/g_{J=0}^{\text{gas}}$ gives the degeneracy ratio at the initial and final states in thermal desorption [24]. $\Delta E^{\text{gas}} = E_{J=1}^{\text{gas}} - E_{J=0}^{\text{gas}} = 14.7$ meV gives the energy difference between the $J = 1$ and $J = 0$ states in the gas phase. It should be emphasized that the desorption intensity ratio given by Eq. (2) does not depend on the energy levels in the adsorption state.

The dot-dashed curve in Fig. 6, obtained from Eq. (2), shows good agreement with the experimental data below 75 K. Above 75 K, on the other hand, the data significantly deviate from the dot-dashed curve, which suggests that the assumption of thermal equilibrium between the $J' = 1$ and $J' = 0$ states via fast o-p conversion does not hold in this region. As discussed above, the desorption energy for $J' = 0$ is lower than that of $J' = 1$ causing preferential desorption of $J' = 0$. If the o-p conversion rate is much faster than the desorption rate, thermal equilibrium between the $J' = 1$ and $J' = 0$ states holds, and so does Eq. (2). When the desorption rate becomes comparable or larger than the o-p conversion rate, on the other hand, Eq. (2) no longer holds. Since the thermal desorption becomes exponentially fast at higher temperatures, the thermal equilibrium may no longer be sustained.

In order to analyze the o-p conversion time, we carried out numerical simulations of TPD for the $J = 1$ and $J = 0$ states taking into account the finite transition probability from $J' = 1$ to $J' = 0$ [27]. We assume that the populations in the respective rotational states approach the thermal equilibrium values determined by Eq. (1) with a transition rate $1/\tau$. We simulate the desorption intensity by changing the desorption energies and frequency factor [27]. In Fig. 6 we show the desorption intensity ratios simulated for various τ values. As we can see in Fig. 6, the results for $\tau = 0.8$ s give a good fit to the experimental data. We are also able to reproduce the TPD curves for $J = 0$ and 1 as shown by the dashed curves in Fig. 3 with desorption energies of 179 and 188 meV, respectively. The deviation at the low-temperature side of the TPD data may be attributed to the presence of another TPD component [16]. Note that the desorption energy difference between the two J states obtained above is reliable within about 1 meV although the desorption energy values depend on the assumed frequency factor [27]. It is worth noting that the equilibrium ortho- H_2 abundance is evaluated to be $\approx 75\%$ at the desorption temperature, which is appreciably larger than the gas phase value at 80 K because of the rotational-energy shift.

Using a two-step model [40], which involves an electron exchange between the adsorbed H_2 and the Pd substrate and nuclear-spin flip via hyperfine interaction to induce o-p conversion, we theoretically calculate the o-p conversion probability. Evaluating the matrix elements for the electron transfer and hyperfine interactions using the DFT-based calculation results, we determine an o-p conversion time $\tau \sim 2$ s at the stable position and orientation [41], which is in agreement with our experimental analysis. We can attribute this substantially fast o-p conversion rate to the strong H_2 -surface electron hybridization as compared to that for H_2 physisorbed on Ag, which is reported to be 2–3 orders of magnitude slower [26,39]. For the accurate estimation of the o-p conversion time, however, calculations taking account of the fluctuation of the molecular orientation and position due to the orientational and zero-point vibrational motion are required [41].

IV. CONCLUSION

Using RS-TPD measurements and theoretical calculations, we determined the rotational state of H_2 and the ortho- H_2 to para- H_2 conversion time in the molecularly chemisorbed state on Pd(210). Due to the highly anisotropic potential that

confines H_2 in the adsorption state, the desorption energy of $H_2(J = 1)$ becomes larger than that of $H_2(J = 0)$. From the desorption intensity ratio of $J = 1$ and $J = 0$ and kinetic simulations of TPD taking account of the o-p conversion, the o-p conversion time is estimated to be of the order of 1 s.

ACKNOWLEDGMENTS

We thank H. Nakanishi, A. Yajima, and S. Yamashita for fruitful discussions, and K. Niki, M. Fujiwara, and T.

Okano for construction of the o-p conversion apparatus. This work was supported in part by JSPS KAKENHI (Grants No. 17H01057, No. 17K19048, No. 17K06818, No. 15KT0062, No. 15K14147, and No. 15H05736) and the NEDO Project “R&D Towards Realizing an Innovative Energy Saving Hydrogen Society based on Quantum Dynamics Applications”. Some of the numerical calculations presented here were done using the computer facilities at the following institutes: CMC (Osaka University), ISSP, KEK, NIFS, and YITP.

-
- [1] E. Ilisca, *Prog. Surf. Sci.* **41**, 217 (1992).
 [2] K. Fukutani and T. Sugimoto, *Prog. Surf. Sci.* **88**, 279 (2013).
 [3] K. Pachucki and J. Komasa, *Phys. Rev. A* **77**, 030501(R) (2008).
 [4] P. Avouris, D. Schmeisser, and J. E. Demuth, *Phys. Rev. Lett.* **48**, 199 (1982).
 [5] S. Andersson and J. Harris, *Phys. Rev. Lett.* **48**, 545 (1982).
 [6] R. E. Palmer and R. F. Willis, *Surf. Sci.* **179**, L1 (1987).
 [7] K. Svensson and S. Andersson, *Surf. Sci.* **392**, L40 (1997).
 [8] S. Li, A. Yu, F. Toledo, Z. Han, H. Wang, H. Y. He, R. Wu, and W. Ho, *Phys. Rev. Lett.* **111**, 146102 (2013).
 [9] F. D. Natterer, F. Patthey, and H. Brune, *Phys. Rev. Lett.* **111**, 175303 (2013).
 [10] F. D. Natterer, F. Patthey, and H. Brune, *ACS Nano* **8**, 7099 (2014).
 [11] S. Li, D. Yuan, A. Yu, G. Czap, R. Wu, and W. Ho, *Phys. Rev. Lett.* **114**, 206101 (2015).
 [12] A. J. Therrien, A. Pronschinske, C. J. Murphy, E. A. Lewis, M. L. Liriano, M. D. Marcinkowski, and E. C. H. Sykes, *Phys. Rev. B* **92**, 161407 (2015).
 [13] A.-S. Mårtensson, C. Nyberg, and S. Andersson, *Phys. Rev. Lett.* **57**, 2045 (1986).
 [14] K. Svensson, L. Bengtsson, J. Bellman, M. Hassel, M. Persson, and S. Andersson, *Phys. Rev. Lett.* **83**, 124 (1999).
 [15] L. Bengtsson, K. Svensson, M. Hassel, J. Bellman, M. Persson, and S. Andersson, *Phys. Rev. B* **61**, 16921 (2000).
 [16] P. K. Schmidt, K. Christmann, G. Kresse, J. Hafner, M. Lischka, and A. Groß, *Phys. Rev. Lett.* **87**, 096103 (2001).
 [17] M. Lischka and A. Groß, *Phys. Rev. B* **65**, 075420 (2002).
 [18] E. Ilisca and F. Ghiglieno, *R. Soc. Open Sci.* **3**, 160042 (2016).
 [19] K. Svensson and S. Andersson, *Phys. Rev. Lett.* **98**, 096105 (2007).
 [20] H. Ueta, N. Watanabe, T. Hama, and A. Kouchi, *Phys. Rev. Lett.* **116**, 253201 (2016).
 [21] T. Sugimoto, Y. Kunisada, and K. Fukutani, *Phys. Rev. B* **96**, 241409 (2017).
 [22] L. Amiaud, A. Momeni, F. Dulieu, J. H. Fillion, E. Matar, and J.-L. Lemaire, *Phys. Rev. Lett.* **100**, 056101 (2008).
 [23] T. Sugimoto and K. Fukutani, *Nat. Phys.* **7**, 307 (2011).
 [24] T. Sugimoto and K. Fukutani, *Phys. Rev. Lett.* **112**, 146101 (2014).
 [25] S. Ohno, M. Wilde, and K. Fukutani, *J. Chem. Phys.* **140**, 134705 (2014).
 [26] K. Fukutani, K. Yoshida, M. Wilde, W. A. Diño, M. Matsumoto, and T. Okano, *Phys. Rev. Lett.* **90**, 096103 (2003).
 [27] See Supplemental Material at <http://link.aps.org/supplemental/10.1103/PhysRevB.97.085436> for a detailed description of sample preparation, DFT calculations for the H_2 potential, theoretical analysis of the rotational state, preparation of para- H_2 , and TPD simulations, which includes Refs. [28–35].
 [28] P. Hohenberg and W. Kohn, *Phys. Rev.* **136**, B864 (1964).
 [29] W. Kohn and L. J. Sham, *Phys. Rev.* **140**, A1133 (1965).
 [30] G. Kresse and D. Joubert, *Phys. Rev. B* **59**, 1758 (1999).
 [31] J. P. Perdew, J. A. Chevary, S. H. Vosko, K. A. Jackson, M. R. Pederson, D. J. Singh, and C. Fiolhais, *Phys. Rev. B* **46**, 6671 (1992).
 [32] J. P. Perdew, K. Burke, and M. Ernzerhof, *Phys. Rev. Lett.* **77**, 3865 (1996).
 [33] H. J. Monkhorst and J. D. Pack, *Phys. Rev. B* **13**, 5188 (1976).
 [34] K. Niki, M. Fujiwara, Y. Motoshima, T. Kawauchi, and K. Fukutani, *Chem. Phys. Lett.* **504**, 136 (2011).
 [35] C. T. Campbell, L. H. Sprowl, and L. Arnadottir, *J. Phys. Chem. C* **120**, 10283 (2016).
 [36] P. Redhead, *Vacuum* **12**, 203 (1962).
 [37] C.-f. Yu, K. B. Whaley, C. S. Hogg, and S. J. Sibener, *J. Chem. Phys.* **83**, 4217 (1985).
 [38] D. White and E. N. Lassertre, *J. Chem. Phys.* **32**, 72 (1960).
 [39] K. Niki, T. Kawauchi, M. Matsumoto, K. Fukutani, and T. Okano, *Phys. Rev. B* **77**, 201404(R) (2008).
 [40] E. Ilisca, *Phys. Rev. Lett.* **66**, 667 (1991).
 [41] E. F. Arguelles *et al.* (unpublished).